Tuijin Jishu/Journal of Propulsion Technology
ISSN: 1001-4055
Vol. 44 No. 3 (2023)

Modified SEPIC Converter Design and Implementation with Grid-Connected PV System in Various Conditions

Syed Faizaan [1], Er. Sonal Sood [2]

[1] M.Tech Scholar, Electrical Engineering Department, Rayat Bahra University, Punjab, India.
Email: syedfaizan918@gmail.com
[2]Assistant Professor, Electronics and Communication Engineering Department
Rayat Bahra University, Punjab

Corresponding Author Email: sonal.sood@rayatbahrauniversity.edu.in

Abstract

Solar energy is becoming increasingly popular due to environmental concerns, government policies and its free availability. However, integrating solar energy into the utility grid presents a significant challenge for researchers due to various factors such as complex electrical equipment, DC/AC conversions, multiple voltage levels, complex grid codes, and the need for accurate modeling techniques. Additionally, improving the performance of solar energy is also important to keep up with other energy production resources. In this paper, a dynamic model of a PV system connected to the grid is presented, which includes a PV array, DC-DC boost converter, voltage source inverter (VSC), transformer, filter, and associated control circuitry. The study also involves the design and implementation of a Modified SEPIC Boost Converter for the system. Simulation results demonstrate improved efficiency and performance of the modified converter compared to the conventional DC-DC boost converter.

Keywords— DC-DC Converter Modified SEPIC topology, low current ripple and high efficiency, on Photovoltaic Applications component.

1. INTRODUCTION

The use of non-renewable energy sources like oil, coal, and other fossil fuels contributes to pollution and climate change, whereas renewable energy sources like solar and wind are considered a solution to mitigate these negative effects. Photovoltaic-based renewable energy is gaining attention as a future energy source because of its ability to solve the problems caused by global warming and the increasing energy consumption. The advantages of photovoltaic energy include being fuel-free, pollution-free, and noise-free, and having a lifespan of up to 20 years, which reduces maintenance costs [1-10]. Before integrating photovoltaic power generation into the grid system, several steps must be taken. Conventional boost converters are typically used to step up the voltage, but they have limitations such as low efficiency, large conduction loss, and high voltage gain [11]. The design and control of the dc-dc boost converter must account for changes in sun irradiance and temperature to ensure a constant voltage supply to the load. The Single-Ended Primary Inductor Converter (SEPIC) is also commonly used to step up the DC voltage level, but the switching voltage stress is higher than that of the Boost converter. The building block of the PV array is the solar cell, which is a p-n semiconductor junction. A photovoltaic source is a current source that depends on the rate of photo-current. Some resistance exists in the path of the electron and is connected in series with the circuit [12-13]. The voltage, current, and power available from a photovoltaic continuously change with variations in sun irradiance and temperature. Therefore, the design and control of the dc-dc

boost converter must ensure a constant voltage supply to the load [14]. To achieve high efficiency, the design of the dc-dc boost converter is a major consideration in renewable power applications [15]. Modified SEPIC boost converters have been shown to reduce voltage oscillations and maintain low current ripple, resulting in high efficiency even when the PV array receives dynamic irradiance [16-19].

2. SYSTEM CONFIGURATION

Fig. 1 shows block diagram of components of a grid-connected PV array system include a PV array, a DC-DC boost converter, a three-phase inverter, a filter, a transformer, and the grid itself.

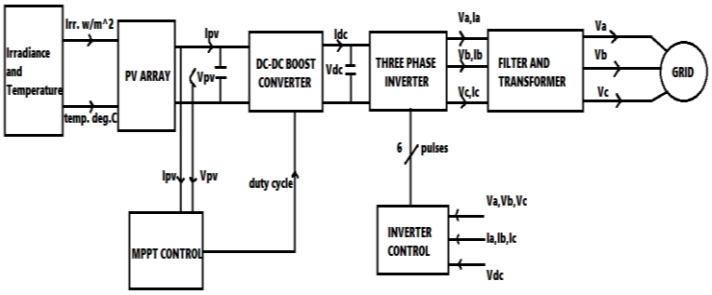

FIG.1. Schematic diagram of Grid connected PV array system with conventional DC-DC boost converter

To ensure better efficiency and minimal distortion in DC voltage during energy conversion, it is important to accurately model the different components of the system and understand their characteristics and dynamic performance. Conventional DC-DC boost converters, such as boost converters, buck converters, and buck-boost converters, typically require high duty cycles to generate high output voltage, leading to high switching voltage stress and inductor current ripple, which negatively impact conversion efficiency and voltage gain [20-21]. Therefore, it is necessary to design a suitable DC-DC boost converter that can effectively control the output voltage, such as the modified SEPIC converter, to improve conversion efficiency.

A. PV Array

The mathematical model of PV array is modeled by considering a single diode equivalent circuit of a PV cell shown in Fig. 2.

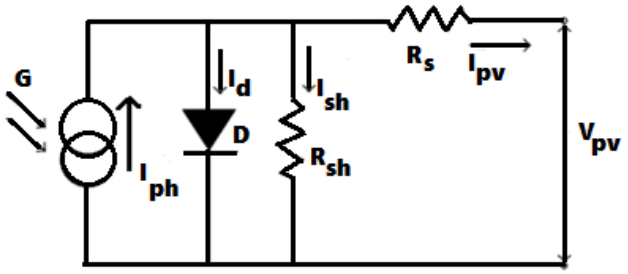

FIG. 2. Equivalent circuit of a PV cell

Equation (1) expresses the output current of an ideal photovoltaic cell as the difference between photon current and diode current. However, a practical PV cell includes series and shunt resistance in addition to the ideal cell. This practical cell can be represented using an equivalent circuit model as shown in fig. 2.

The current of the PV cell is given by the equations given as;

$$I_{PV} = I_{ph} - I_d - I_{sh} \qquad (1)$$

$$I_d = I_s\,(e^{\frac{q(V_{PV}+R_S I)}{mKT}} - 1) \qquad (2)$$

$$I_{sh} = \frac{V_{PV}+IR_S}{R_{sh}} \qquad (3)$$

By putting (2) and (3) in (1), I_{PV} can be given as:

$$I_{PV} = I_{ph} - I_s\left(e^{\frac{q(V_{PV}+R_S I)}{mKT}} - 1\right) - \frac{V_{PV}+IR_S}{R_{sh}} \qquad (4)$$

The output power P_{PV} of the photovoltaic cell is given by:

$$P_{PV} = V_{PV} I_{PV} \qquad (5)$$

Where,

- I_d denotes the diode current
- I_{ph} denotes the photon current
- I_{PV} denotes the cell current
- I_s denotes the saturation current of diode
- q denotes the electrical charge
- m denotes the ideality factor
- T denotes the cell temperature in Kelvin
- K denotes the Boltzmann constant
- V_{PV} denotes the terminal voltage of the array
- R_s denotes the series resistance
- R_{sh} denotes the shunt resistance

- ***Characteristics of PV cell***

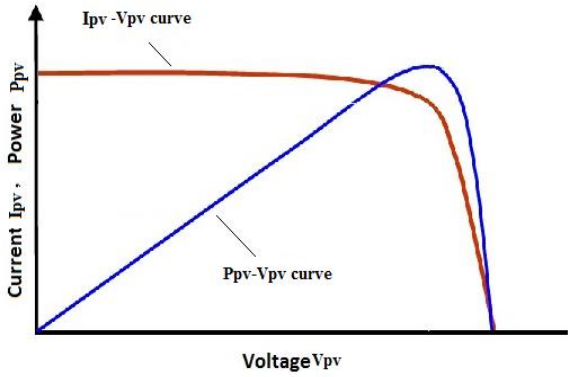

FIG 3. Characteristics of PV cell

The mathematical model for the PV array is developed by incorporating equations (1) to (5), considering the number of series and parallel cells and its corresponding losses in terms of resistances.

B. DC-DC Boost Converter

The circuit depicted in Fig. 4 is designed to function in a continuous conduction mode, which means that it operates in a cyclical manner between two loops. When the switch is in the "ON" state, the inductor current increases, and energy is stored in it. Simultaneously, the capacitor C discharges through the load resistor R, following a specific relationship:

$$L\frac{di_L}{dt} = V_{PV} \quad (6)$$

$$C\frac{dV_{dc}}{dt} = \frac{V_{dc}}{R} \quad (7)$$

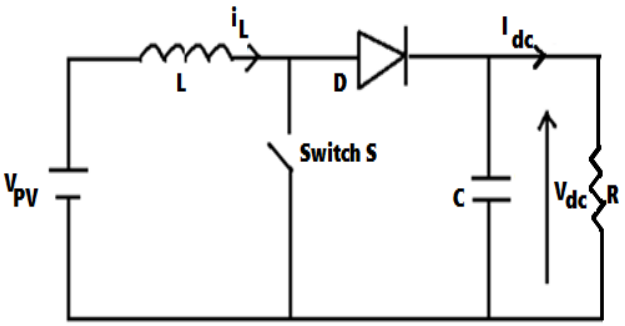

FIG. 4. Circuit diagram of conventional DC-DC boost converter

On the other hand, when the switch is turned off, the stored energy in the inductor is supplied to the load. During this time, the inductor current decreases, and the output capacitor voltage increases. These changes can be described using the following equations:

$$L\frac{di_L}{dt} = V_{PV} - V_{dc} \quad (8)$$

$$C\frac{dV_{dc}}{dt} = i_L - \frac{V_{dc}}{R} \quad (9)$$

In a conventional boost converter, the voltage across the inductor increases when the switch is on and it decreases when the switch is off, resulting in the charging of the output capacitor through the diode. The inductor current does not fall to zero in continuous conduction mode. The duty cycle of the converter is controlled by the MPPT controller. The duty cycle equation for the conventional boost converter can be expressed as:

$$\text{Duty cycle,} \quad d = \frac{V_{PV} - V_{dc}}{V_{dc}} \quad (10)$$

- ***Modified SEPIC converter***

The modified SEPIC converter is created by integrating the conventional SEPIC converter with a DC-DC boost converter and a diode-capacitor circuit [19].

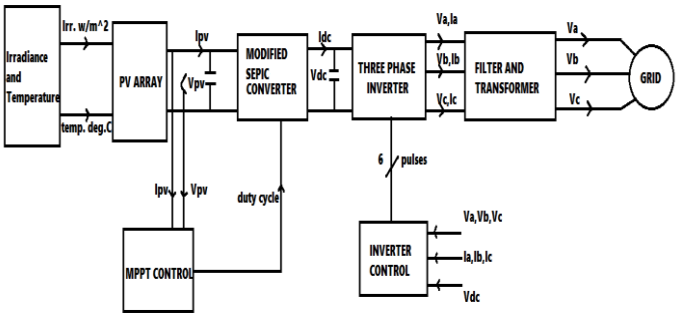

FIG. 5. Schematic diagram of grid connected PV array system with modified SEPIC converter

The modified SEPIC converter is designed by combining a conventional SEPIC converter with a DC-DC boost converter and a diode-capacitor circuit. This converter is suitable for PV systems and provides high efficiency, low current ripple, low switching voltage stress, and low conduction losses. By introducing a

diode-capacitor circuit in series and using low voltage rating MOSFET and low resistance, the voltage stress across MOSFET and diodes is reduced, increasing the conversion efficiency of the proposed model. The proposed converter topology is appropriate for renewable energy-based applications with low input DC voltage. The circuit topology of the proposed converter is shown in Fig. 6, which includes a DC voltage source V_{dc}, main switch S, three diodes D_1, D_2, and D_3, three capacitors C_1, C_2, and C_3, two inductors $L_1$and L_2, output diode D_0, and output capacitor C_0. To increase the static voltage gain, the diode-capacitor based SEPIC converter is proposed with a combination of a boost converter. The diode-capacitor elements help reduce stress on the switch, and the capacitor is charged with the output voltage of the converter. The voltage from the capacitor C_2 is applied to the inductor L_2 during the conduction period of power switch S, which increases the voltage gain [22], compared to a conventional DC-DC boost converter.

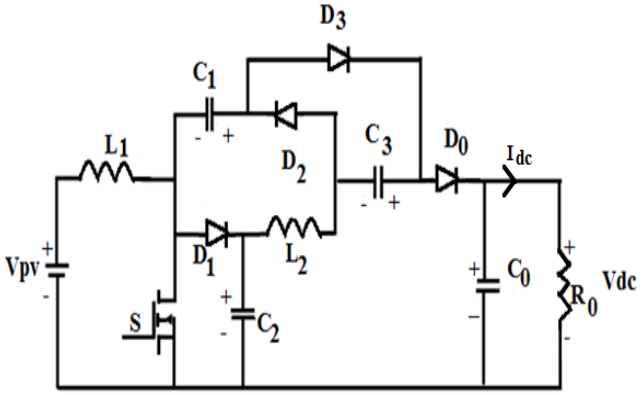

FIG. 6. Circuit diagram for modified SEPIC converter

- ***Parameter calculations of Modified SEPIC converter***

  Table no. 1:

Parameters	***Conventional Boost converter[22]***	***Modified SEPIC Boost Converter[21]***
Duty cycle	$\boldsymbol{d = 1 - \frac{V_{PV}}{V_{dc}}}$	$\boldsymbol{D = \frac{2V_{dc} - 3V_{PV}}{2V_{dc} + V_{PV}}}$
Inductors	$\boldsymbol{L_1 = \frac{V_{dc} d}{\Delta i_L f_s}}$	$\boldsymbol{L_1 = \frac{V_{PV} D}{\Delta i_{L1} f_s}}$ $\boldsymbol{L_2 = \frac{V_{c2}(1 - D)}{\Delta i_{L2} f_s}}$
Capacitors	$\boldsymbol{C = \frac{d}{R\frac{V_{dc}}{V_{PV}} f_s}}$	$\boldsymbol{C_1 = C_2 = C_3 = \frac{I_{dc}}{\Delta V_c f_s}}$

- V_{PV} denotes the input voltage that is 273V
- V_{dc} denotes the output voltage that is 500V
- f_s denotes the fundamental frequency that is 5×10^3Hz
- D denotes the duty cycle for modified SEPIC converter

- d denotes the duty cycle for conventional DC-DC boost converter
- ΔV_c denotes the voltage ripple on capacitor C_1, C_2, C_3

- $\Delta i_{L1,2}$ denotes the ripple current on inductor L_1, L_2
- L_1, L_2 denotes the inductance of modified SEPIC converter
- C_1, C_2, C_3 denotes the capacitance of modified SEPIC converter

C. Three - Phase Inverter

A three-phase inverter comprises three single-phase inverter switches. The switches are controlled in a coordinated manner to ensure that one switch operates at each 60-degree point of the fundamental output waveform, resulting in a line-to-line output waveform with six steps. The six-step waveform has a zero-voltage step between the positive and negative sections of the square-wave, which eliminates the harmonics that are multiples of three. By applying SPWM techniques to six-step waveforms, the waveform's overall shape, or envelope, is preserved, resulting in the cancellation of the 3rd harmonic and its multiples.

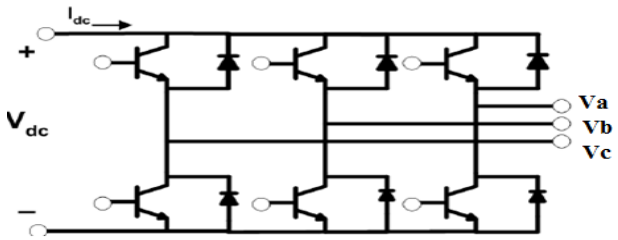

FIG. 7. Circuit diagram of three phase inverter

D. Control Techniques

- ***MPPT control mechanism for converter***

The power-voltage curve of a solar panel indicates that there exists an optimal operating point at which the maximum power can be delivered to the load.

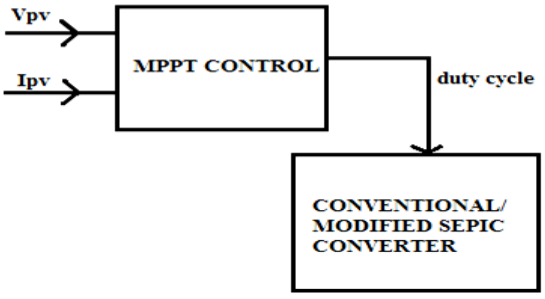

FIG. 8. MPPT Control structure diagram of conventional/modified SEPIC converter

This operating point varies with changes in solar irradiation and cell temperature and needs to be regulated [23]. The control structure diagram for regulating the operating point is shown in Fig. 8.

- ***Incremental conductance***

The incremental conductance method involves the use of two sensors, one to measure the voltage and the other to measure the current output of the PV array [24]. The effectiveness of the overall PV system is influenced by both the DC-DC converter utilized and the MPPT algorithm employed, as both of these factors can enhance the

performance of the PV array [25]. Differentiating equation (5) with respect to voltage yields the following equation:

$$\frac{dP_{PV}}{dV_{PV}} = V_{PV} \times \left(\frac{dI_{PV}}{dV_{PV}}\right) \quad (11)$$

$$\frac{dP_{PV}}{dV_{PV}} = I + V_{PV} \times \left(\frac{dI_{PV}}{dV_{PV}}\right) \quad (12)$$

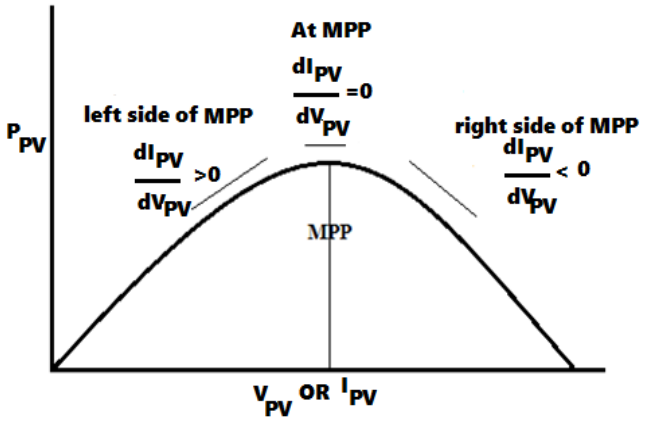

FIG. 9. Incremental conduction realization

The condition for maximum power point tracking is that the slope $\frac{dP_{PV}}{dV_{PV}}$ should be equal to zero. Substituting this condition in (11), the equation becomes:

$$\frac{dI_{PV}}{dV_{PV}} = -\left(\frac{I_{PV}}{V_{PV}}\right) \quad (13)$$

The relation is given by the following equations:

At MPP:

$$\frac{dI_{PV}}{dV_{PV}} = -\frac{I_{PV}}{V_{PV}} \quad (14)$$

Left of MPP:

$$\frac{dI_{PV}}{dV_{PV}} > -\frac{I_{PV}}{V_{PV}} \quad (15)$$

Right of MPP:

$$\frac{dI_{PV}}{dV_{PV}} < -\frac{I_{PV}}{V_{PV}} \quad (16)$$

Where I_{PV} and V_{PV} are PV array output current and voltage respectively. The left-hand side of this equation represents the incremental conductance of the PV module, while the right-hand side represents the instantaneous conductance. The solar array will operate at the maximum power point when the ratio of the change in output conductance is equal to the negative output conductance. The performance of the PV system depends on the type of DC-DC converter used and the algorithm used for tracking the MPPT.

- ***Control mechanism for three phase inverter***

A three-phase three-level system is designed using IGBT switches to link the inverter to the network. The use of IGBT semiconductor is preferred because of its smaller size and lower switching losses compared to other power electronic devices. VSC regulates the DC bus voltage and also maintains a unity power factor. Figure 10 illustrates the control mechanism for the three-phase inverter. [26].

- ***DC link voltage control***

The DC link capacitor plays an important role in compensating for power losses in the inverter IGBT switches, thereby providing real power. As a result, the voltage of the DC link capacitor decreases gradually over time. In order to maintain the capacitor voltage at a stable level, the inverter must absorb a small amount of active power. This concept has been discussed in several studies [27-28].

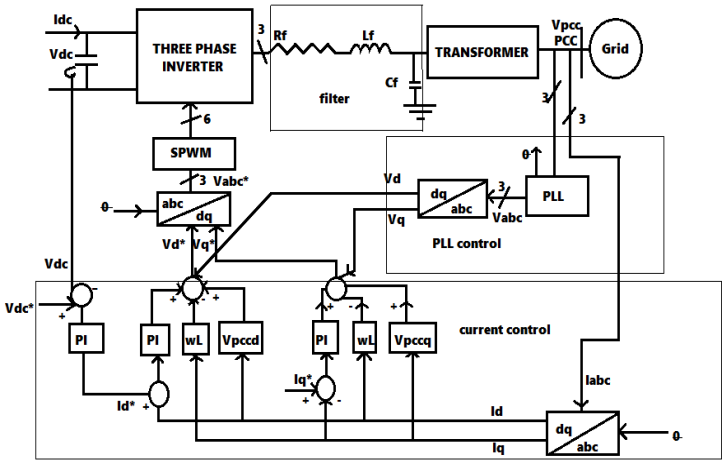

FIG. 10. Control mechanism for three phase inverter

- ***Phase locked loop***

To control the output voltage in a power electronic system, the phase locked loop (PLL) technique is commonly used to synthesize the system's phase and frequency. The PWM technique is used in conjunction with PLL to achieve this. The q component of the Point of Common Coupling (PCC) voltage in the d q-frame [29] can be expressed as follows:

$$V_{pcc-q} = \hat{V} \sin(\omega t + \theta_0 - \theta) \qquad (17)$$

To decouple the active and reactive power controls, V_{pcc-q} is regulated to zero. This is because the active power control is related to the real part of the output voltage, which is in-phase with the grid voltage, and the reactive power control is related to the imaginary part of the output voltage, which is 90 degrees out of phase with the grid voltage. By regulating to zero, the output voltage will have only the in-phase component with the grid voltage, which is necessary for active power control, and the out-of-phase component will be eliminated, making it possible to control only the reactive power. In the given equation $\hat{V}$ denotes the amplitude of PCC phase voltage, ω is the system frequency and θ_0 is initial phase angle of the AC system.

- ***Current control***

The inverter current in dq- frame are given by equations [31], [28]:

$$L_f \frac{di_d}{dt} = L_f \omega(t) i_q - R_f i_d + V_d - V_{pcc-d} \qquad (18)$$

$$L_f \frac{di_q}{dt} = -L_f \omega(t) i_d - R_f i_q + V_q - V_{pcc-q} \qquad (19)$$

Where V_{pcc-dq} denotes PCC voltages, i_{dq} is inverter current, V_{dq} is the voltage at AC side of the inverter in dq-frame, respectively. A PI controller is used for each current component [30]. The active and reactive power outputs of the inverter in dq-frame are given by the equations:

$$P(t) = \frac{3}{2}(V_q(t) i_d(t) + V_d(t) i_q(t) \qquad (20)$$

$$Q(t) = \frac{3}{2} (-V_d(t) i_q(t) + V_q(t) i_d(t)) \qquad (21)$$

Due to PLL operation $V_d = \hat{V}$ and $V_q = 0$.

The current controllers of the inverter receive reference values from outer loops, which are based on the operation mode and control objectives. The active power output of the inverter is controlled by regulating i_d, while the reactive power output is regulated by i_q.

3. RESULTS AND DISCUSSIONS

The equations for both conventional and modified boost converters have been solved using the Tustin/Backward Euler method in MATLAB/SIMULINK. The simulation has been carried out for the PV array under standard test conditions (25°C, 1000 W/m^2) for a duration of 0.4 seconds. The same model has been simulated for the modified SEPIC boost converter, which was designed based on the parameters given in Table 1 and values provided in Table 2, under the same standard test conditions and time.

4. COMPARATIVE ANALYSIS OF CONVENTIONAL AND MODIFIED SEPIC BOOST CONVERTER

In Figure 11, it can be observed that the grid power P, in the case of the modified SEPIC converter, becomes stable prior to the output power in the case of the conventional boost converter. Additionally, the output power of the modified SEPIC converter is higher than that of the conventional converter. Furthermore, the efficiency comparison of the power of the grid-connected system with conventional and modified SEPIC converters is shown in Figure. It can be easily observed that during the time period of 0.2-0.4 seconds, the designed converter has a higher efficiency of 96.2%. This is because changes in temperature or irradiance affect the design of the conventional boost converter, which generates ripples in the DC output voltage. On the other hand, the influence of capacitors, diodes, and inductances keeps the output of the modified SEPIC converter smooth, with low voltage ripple and high efficiency [22-30].

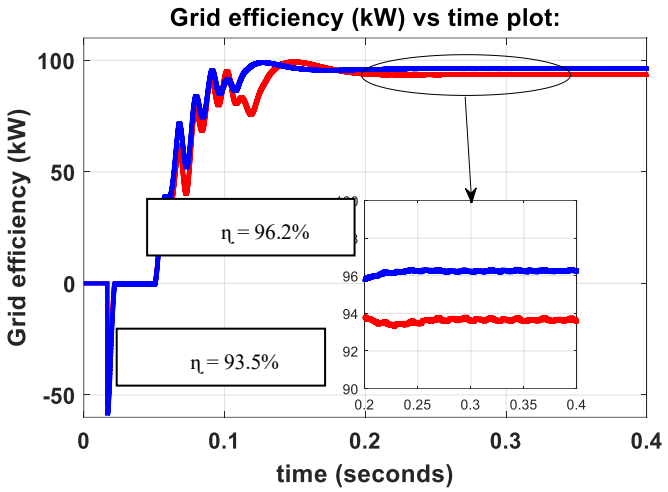

FIG. 11. Comparative analysis of grid power P with conventional and modified SEPIC converter

Figures 12 and 13 shows the calculation of Total Harmonic Distortion (THD) on the grid side for both conventional and modified SEPIC converters. It can be observed from the figures that the THD calculated for both converters is the same, i.e., 0.33%.

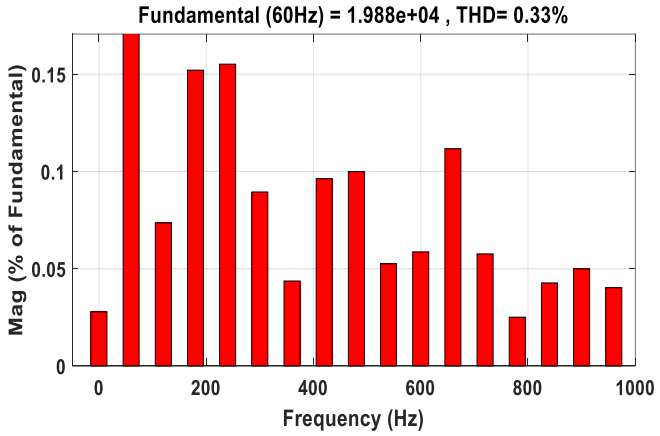

FIG. 12. THD in case of Conventional boost converter

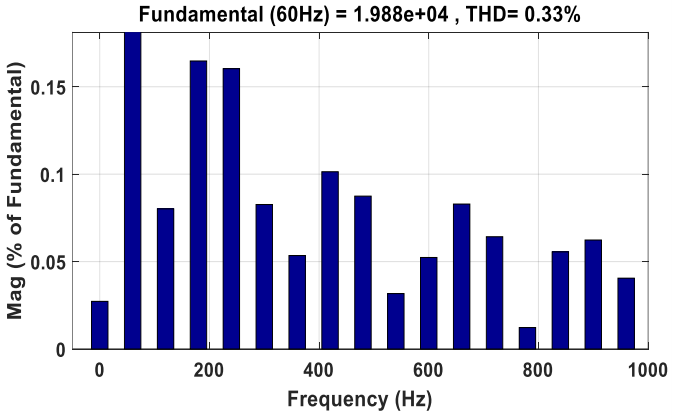

FIG. 13. THD in case of modified SEPIC converter

Alternatively, the performance of conventional and modified SEPIC boost converter is summarized in following table:

Table no. 1:

S.no	***Performance parameters***	***Conventional boost converter***	***Modified SEPIC boost converter***
1.	*Efficiency*, η	*93.5%*	*96.2%*
2.	*THD*	*0.33%*	*0.33%*

5. CONCLUSIONS

In addition to the detailed modeling of the power circuit and associated control circuitry of the grid-connected PV system, the main conclusions of this work are:

- The efficiency of the grid-connected PV system with the conventional boost converter is 93.5%, while the efficiency of the same system with the designed boost converter is 96.2%.
- The voltage profile of the system during the transient period with the proposed modified SEPIC converter is improved compared to the voltage profile of the system with the conventional DC-DC boost converter.
- The total harmonic distortion (THD) of the voltage being fed to the utility grid is 0.33%, which is the same for the system with both converters.

REFERENCES

[1] Nehrir MH, Wang C, Strunz K, Aki H, Ramakumar R, Bing J, Miao Z, Salameh Z, "A review of hybrid renewable/alternative energy systems for electric power generation: Configurations, control and applications," *IEEE Trans. Sustain. Energy*, vol. 2, no. 4, pp. 392–403, Oct. 2011.

[2] Benjamin Kroposki, Robert Lasseter, Toshifumi Ise, S. Morozumi, S. Papathanassiou, and N. Hatziargyriou, "Making Microgrids Work", *IEEE Power and Energy Magazine*, vol.6, no.3, pp. 41-53, May-June 2008.

[3] Chi Kong Tse and Kevin M. Adams, "Qualitative analysis and control of a DC-to-DC Boost Converter Operating in Discontinuous Mode", *IEEE Transactions on Power Electronics*, Vol. 5, No. 3, pp 323-330, July 1999.

[4] Dieter K. Schroder, "Carrier Lifetimes in Silicon" *IEEE Transactions on electron devices*, 44 (1), pp 160-170, Apr. 1997.

[5] Peyman Mazidi and G. N. Srinivas; "Reliability assessment of a distributed generation connected distribution system". International Journal of Power System Operation and Energy Management, 2011.

[6] Ministry of New and Renewable Energy, Government of India, "Annual Reports 2016-2017" , 2016, [Online], Available: http://mnre.gov.in/filemanager/annual-report/2016-2017/EN/pdf/1.pdf, [Accessed: July 6, 2017].

[7] "Ministry of New and Renewable Energy, Annual Report 2015-2016."

[8] Clemente Rodriguez, Gehan Amaratunga, "Dynamic stability of grid-connected photovoltaic systems," *IEEE Power Engineering Society General Meeting*, pp. 2193-2199, June 2004.

[9] Mohamad Reza Banaei and Hossein Ajdar Faeghi Bonab, ‘‘A novel structure for single-switch nonisolated transformerless buck–boost DC–DC converter,’’ *IEEE Trans. Ind. Electron.*, vol. 64, no. 1, pp. 198–205, Jan. 2017.

[10] Coelho, Roberto F., Filipe Concer, and Denizar C. Martins. "A study of the basic DC-DC converters applied in maximum power point tracking." In Power Electronics Conference, 2009. COBEP'09. Brazilian, pp. 673- 678. IEEE, 2009.

[11] W. Li and X. He, “Review of non- isolated high-step-up dc/dc converters in photovoltaic grid-connected applications”, *IEEE Trans. Ind. Electron*., vol. 58, no. 4, pp. 1239–1250, Apr-2011.

[12] Y.Tan, et al., “A model of PV generation suitable for stability analysis,” Energy conversion, *IEEE Transactions on*, vol.19, pp. 748-755, 2004.

[13] Marcelo Gradella Villalva and Jonas Rafael Gazoli, "Comprehensive approach to modeling and simulation of photovoltaic arrays," Power Electronics, *IEEE Transactions on*, vol. 24, pp. 1198- 1208,2009.

[14] Jong. Pil Lee, Byung-Duk Min, Tae-Jin Kim, Dong-Wookyoo and Ji-Yoon Yoo, “Input Series-output parallel connected DC/DC converter for a photovoltaic PCS with high efficiency under a wide load range”, Journal of Power Electronics, vol. 10, No.1, pp.9-13, January 2010.

[15] A.W.N. Husna, S.F. Siraj, M.Z. Ab Muin, “Modeling of DC-DC converter for solar energy system applications”, *IEEE Symposium on Computers & Informatics*, pp. 125-129, Mar. 2012.

[16] Daniel WH. Power Electronics. Indiana: McGraw-Hil. 2011: 144-150.

[17] Falin J. Designing DC / DC Converters Based on SEPIC Topology. Analog Appl J. 2008; 18–23.

[18] Kircioğlu O, Ünlü M, Çamur S. *Modeling and Analysis of DC-DC SEPIC Converter with Coupled Inductors*. 2016 International Symposium on Industrial Electronics, INDEL 2016 Proceedings. Bosnia Herzegovina. 2016: 1-5.

[19] Saravanan S, Babu NR. Design and Development of Single Switch High Step-up DC-DC Converter. *IEEE J Emerg Sel Top Power Electron*. 2017; 6(2): 855-863.

[20] Lung-Sheng Yang, Tsorng-Juu Liang, and J. F. Chen, “Transformer-less DC-DC converter with high voltage gain”, *IEEE Trans. Ind. Electron*., vol. 56, no. 8, pp. 3144–3152, Aug. 2009.

[21] R. Gules, W. M. Santos, F. A. Reis, E. F. R. Romaneli, and A. A Badin, “A modified SEPIC converter with high static gain for renewable applications,” *IEEE Trans. Power Electron*., vol. 29, no. 11, pp. 5860-5871, Nov. 2014.

[22] Daniel WH. Power Electronics. Indiana: McGraw-Hil. 2011: 144-150.

[23] Carl Ngai-Man Ho, Hannes Breuninger, SamiPettersson, Gerardo Escobar, Leonardo Augusto Serpa, and Antonio Coccia, “Practical design and implementation procedure of an interleaved boost converter using SiC diodes for PV applications,” *IEEE Trans. on power electronics*, vol.27, no. 6, June 2012.

[24] Azadeh Safari and Saad Mekhilef, "Simulation and Hardware implementation of incremental conductance MPPT with direct control method using Cuk converter", *IEEE Trans.Ind. Electron.*, Vol . 58, no. 4, Apr. 2011, pp. 1154-1161.

[25] M. Veerachary, T. Senjyu, K. Uezato, (2002), “Voltage-based maximum power point tracking control of PV system”, Aerospace and Electronic Systems, *IEEE Transactions on ower electronics* , vol. 38, no. 1, 2002, 262- 270.

[26] Linbin Huang, “A Virtual Synchronous Control for Voltage-Source Converters Utilizing Dynamics of DC-Link Capacitor to Realize Self Synchronization”, *IEEE J. Emerg. Sel. Top. Power Electron*, vol. 5, no. 4, pp. 1565–1577, 2017.

[27] A. Yazdani and R. Iravani, Voltage-Sourced Converters in Power Systems: Modeling, Control, and Applications. New York, NY, USA: Wiley, 2010.

[28] A. Yazdani et al., "Modeling guidelines and a benchmark for power system simulation studies of three-phase single-stage photovoltaic systems," *IEEE Trans. power delivery*, vol. 26, no. 2, pp. 1247–1264, Apr. 2011.

[29] Best, Roland E. Phase-Locked Loops: Design, Simulation, and Application. McGraw-Hill, (Fifth Edition) 2003.

[30] E. M. Siavashi, "Smart PV inverter control for distribution systems," Electron. Thesis Dissertation Repository, 3065, 2015. [Online]. Available: https://ir.lib.uwo.ca/etd/3065